

Seasonal variation of CO₂ flux and its environmental factors in evergreen coniferous plantation

LIU Yunfen¹, SONG Xia^{1,2}, YU Guirui¹, SUN Xiaomin¹, WEN Xuefa^{1,2}
& CHEN Yongrui¹

1. Institute of Geographic Sciences and Natural Resources Research, Chinese Academy Sciences, Beijing 100101, China;

2. Graduate School of the Chinese Academy of Sciences, Beijing 10039, China

Correspondence should be addressed to Liu Yunfen (email: liuyf@igsnrr.ac.cn)

Received July 14, 2004; revised January 19, 2005

Abstract The effects of environmental factors on carbon flux were analyzed, the spatial and temporal variation of carbon flux was studied at the two heights of 23 m and 39 m with the eddy covariance technique, and the carbon budget was evaluated for evergreen coniferous plantation in the red earth hilly area during the year 2003. The results showed that photosynthetically active radiation (PAR) and soil temperature are essential factors strongly affecting the net ecosystem exchange (NEE); in the daytime, the response of NEE to PAR shows a rectangular hyperbola trend, and in the nighttime, the significant correlation was observed between soil temperature and soil respiration which was filtered using friction velocity. This ecosystem appeared as a carbon sink along the whole year of 2003, and the carbon flux showed the obvious seasonal fluctuation and diurnal variability. The seasonal peak of NEE occurred in May and June with the daily sum about $0.61\text{--}0.67\text{ mg} \cdot \text{CO}_2 \cdot \text{m}^{-2} \cdot \text{s}^{-1}$. For the severe drought in the mid-summer, the daily sum was $0.40\text{--}0.44\text{ mg} \cdot \text{CO}_2 \cdot \text{m}^{-2} \cdot \text{s}^{-1}$ in July which was only 2/3 of that in the last two months. For the lasted drought of the year, the nadir of NEE happened in the winter with the daily sum about $-0.29\text{ to }-0.35\text{ mg} \cdot \text{CO}_2 \cdot \text{m}^{-2} \cdot \text{s}^{-1}$. The sink intensity of the ecosystem was about $-0.553\text{ to }-0.645\text{ kg} \cdot \text{Cm}^{-2}$ per year in 2003.

Keywords: net ecosystem exchange, eddy covariance, coniferous plantation, red earth hilly area.

DOI: 10.1360/05zd0012

The net carbon balance of ecosystem has been and will still be the focus for global change research. However, accurate estimating soil-vegetation-atmosphere carbon flux is the keystone for discovering the processes of regional carbon sink/source. FLUXNET, a global network of micrometeorological tower sites, uses eddy covariance techniques to measure the exchange of carbon dioxide, water vapor, and energy between ecosystem and atmosphere, accordingly, ChinaFLUX was created in 2002 with the goals: (1) to

understand the impact factors for carbon exchange and its related processes including soil processes, vegetation structure, physiological processes related to CO₂ in the different growing stages; and (2) to determine the principal feedbacks that may affect the biosphere under the future climate, such as responses to climate changing, air pollution, and CO₂ enhancement. The ChinaFLUX covers the main typical ecosystems in China, the forest ecosystem including temperate coniferous and broad mixed forest, subtropical conifer-

Copyright by Science in China Press 2005

ous plantation, subtropical typical evergreen broad forest, and tropical seasonal rain forest. The Qianyanzhou station belongs to subtropical coniferous plantation, which represents the typical recovery ecosystem. Totally there is about $45 \times 10^4 \text{ km}^2$ homogeneous ecosystem. To exactly estimate the net productivity and responses to global change of this ecosystem is useful for investigating the roles of human disturbance, and could provide a sound base for evaluating the impact of plant recovery to ecological environments.

In recent years, the eddy covariance technique has emerged as an efficient way to assess ecosystem carbon exchange^[1-4], and it has become an standard method for the FLUXNET (Ameri-Flux, Euro-Flux, Asia-Flux, Ko-Flux, Oz-Flux, Canada-Flux). The eddy covariance technique has the potential for directly measuring the net flux density of carbon dioxide between patches of landscape and the atmosphere. The horizontal length scale of these measurement ranges from 100 m to several kilometers. Temporally, the eddy covariance technique can involve time intervals ranging from hours to days through seasons and years^[5]. The ideal condition of eddy covariance technique is homogeneous upwind fetch and stationary, homogeneous mixing turbulent. However, most of the terrains is heterogeneous in fact, for the complex terrain of the Qianyanzhou station, we installed the instruments at two heights of 23 m and 39 m in order to evaluate the carbon budget of this ecosystem exactly. The object of this paper is to analyze the seasonal variation of carbon flux and the response of carbon flux to environmental factors based on the whole year observed data in the year 2003.

1 Sites and material

1.1 Sites description

Qianyanzhou flux tower ($26^\circ 44' 29.1''\text{N}$, $115^\circ 03' 29.2''\text{E}$), set up in August 2002, is located in the Qianyanzhou Agriculture Experimental Station of Red Soil and Hilly Land of CERN, CAS. The region has a hilly topography with a slope ranging between 2.8° and 13.5° . The forest coverage is about 90% around the tower, with splash pine in the west, masson

pine in the southeast, and Chinese fir dominating in the northeast. The mean canopy height is approximately 12 m, about 20 years old. According to the wind tunnel studies, flux measurements should be made at 2—3 times height of the trees, and the measuring heights are 23 m and 39 m in this research. The two eddy covariance systems consist of three-dimensional sonic anemometers (CSAT3, Campbell Scientific Ltd, USA) for wind speed and temperature, and infrared gas analyzer (Li-7500, LI-Cor Inc, USA) for CO_2 and water vapor concentrations. In addition, there are seven level CO_2 profile system (LI-820, Li Cor Inc, USA) and routine meteorological measurement system, installed at 1.6, 7, 11, 15, 23, 31, 39 m respectively, the global radiation, net radiation and PAR sensors installed at 41 m, infrared thermometer installed at 2 m and 41 m, the soil temperature sensors installed at 0, 1, 5, 20, 50, and 100 cm, the soil moisture sensors installed at 5, 20, and 50 cm, and the soil heat flux plate installed at 3 cm and 5 cm. Data were digitally logged continuously over 30 min periods at a 10 Hz rate and recorded for post-processing at which time final flux computations were made. The PC card and desk computer can log the data at the same time. The collected data includes Ts-data (10 Hz), half-hourly data (mean data every 30 min), and daily data (mean data every day). Song has described the site condition and the instruments in detail^[6].

1.2 Methods

The eddy covariance, applied in this study, measures the flux directly through the fluctuation of wind velocities and scalar density, so that the eddy covariance technique is a method to directly measure the $\text{CO}_2/\text{H}_2\text{O}$ and energy flux between vegetation and atmosphere^[7]. The eddy covariance technique is based on the conservation of mass^[7,8]; it is assumed that in the unit volume the changing rate of CO_2 density is the sum of the vertical divergence, horizontal latitudinal advection, horizontal longitudinal advection, and the biological production or consumption.

The flux is the instantaneous amount of material passing through a horizontal plane of unit area per unit time. According to Reynolds' averaging procedures,

the average of fluctuations about a mean and the mean vertical velocity over a horizontal, homogeneous extended surface are zero, so the mean vertical turbulent flux of material over a horizontally homogeneous surface under steady-state condition is^[9]

$$Fc = \overline{wc} = \overline{w'c'} + \overline{wc}, \quad (1)$$

where Fc is the flux of scalar gas c , c is the scalar gas density, w is the vertical velocity, overbars denote time averaging and primes denote fluctuations from the mean, furthermore, over a horizontally homogeneous surface, the last term in above equation is negligible, so the flux can be expressed by the covariance of the fluctuation of vertical velocity and the density of scalar gas; Fc is assumed the scalar gas flux of averaging time, and $w'c'$ is the instantaneous amount of material passing through a plane^[10]. Therefore we can attain the sensible flux, momentum flux, CO₂ flux and vapor gas flux, the following is the equations:

$$H = \rho C_p \overline{w'\theta'}, \quad (2)$$

$$T = \rho \overline{w'u'}, \quad (3)$$

$$C = \rho \overline{w'c'}, \quad (4)$$

$$E = \rho C_p \overline{w'q'}, \quad (5)$$

where C_p is specific heat at constant pressure, θ' is potential temperature fluctuations from the mean, u' is the wind speed component fluctuations from the mean in the horizontal direction, q' is the density fluctuation of vapor gas specific humidity. All of above expressions are the essential equations of eddy covariance technique, so we can attain the flux when we measure the density fluctuation of material.

The net ecosystem exchange (NEE) is the difference between the sum of carbon uptake in the photosynthesis, the storage carbon below the height of observation and the carbon emission through the autotrophic and heterotrophic respiration^[11], so the NEE of a scalar constituent with the atmosphere should be

$$NEE = Fc + F_{\text{storage}} = \text{NPP} - R_{\text{eco}}, \quad (6)$$

where Fc is the carbon flux between vegetation and atmosphere, F_{storage} is the carbon storage below the measurement height, NPP is the net primary productivity, R_{eco} is the ecosystem respiration.

Assuming that there is no divergence of horizontal eddy flux and no horizontal advection, eq. (6) is

$$NEE = \int_0^z \frac{\partial \bar{c}}{\partial t} dz + (\overline{w'c'})_r + \overline{wr}(\bar{c}_r - \langle \bar{c} \rangle), \quad (7)$$

where subscript r denotes a quantity at height zr and $\langle \bar{c} \rangle$ is the averaged concentration between the ground and this height. eq. (7) shows that NEE should consist of three components, storage below the height of observation (term 1), eddy flux (term 2) and a mass flow component arising from the horizontal flow divergence/convergence or a non-zero mean vertical velocity (term 3), the last term, somewhat analogous to a bulk heat deficit term due to nocturnal subsidence, can be understood by considering a volume of air over the eddy covariance footprint^[4]. As the experimental condition, we just consider the first two terms (it may cause the underestimate of NEE).

2 Data processing

2.1 CO₂ gas density correction

CO₂ is measured using infrared spectrometers, so the CO₂ concentration was expressed as molar density, ρ_c (moles per unit volume), not mixing ration, c . In theory, changes in molar density can occur by adding or removing molecules in a controlled volume or by changing the volume, as is done when pressure, temperature and humidity change in the atmosphere. By measuring the eddy flux covariance in terms of molar density, the net flux density of CO₂ across the atmosphere-biosphere interface is evaluated as

$$F = \overline{w\rho_c} = \overline{w'\rho'_c} + \overline{w\rho_c}, \quad (8)$$

the first term on the right hand side of eq. (8) is the product of the mean vertical velocity and CO₂ density. The mean vertical velocity arises from density fluctuations. Its magnitude is too small ($< 1 \text{ mm s}^{-1}$) to be detected by anemometry^[12], but it can be computed on

the basis of temperature (T) and humidity density (ρ_v) fluctuations using the Webb-Pearman-Leuning algorithm:

$$Fc = \overline{w' \rho_c'} + \frac{m_a}{m_v} \frac{\overline{\rho_c}}{\overline{\rho_a}} \overline{w' \rho_v'} + \left(1 + \frac{\overline{\rho_v m_a}}{\overline{\rho_a m_v}} \right) \frac{\overline{\rho_c}}{T} \overline{w' T'}, \quad (9)$$

where m_a is the molecular weights of air, m_v is the molecular weights of water vapor. Eq. (9) ignores effects of pressure fluctuations, which may be significant under heavy winds^[13] and advection^[8]. Significant terms in eq. (9) depend on whether one uses an open or closed path infrared spectrometer. If one draw air down a heated tube in a turbulent state, as is needed to implement a closed-path sensor, temperature fluctuations will dampen and approach zero, thereby canceling the last term on the right hand side of eq. (9)^[14,15]. In this study, the fluctuation of CO₂ density caused by temperature and vapor gas is corrected.

2.2 Coordinate rotation

Over sloping terrain, the mean vertical velocity, with respect to the geographic potential, will be non-zero because hills cause wind streamlines to converge and diverge^[16]. Classically, investigators apply a mathematical rotation to the wind coordinate system to compute flux covariance^[7,17,18]. If meso-scale circulations persist, it is inappropriate to rotate the coordinate system and force the mean vertical velocity to zero^[19]. A new reference for coordinate rotation must be defined and it depends on wind direction, instrument biases and the slope of the upwind terrain^[8]. With this modification, the net ecosystem exchange of CO₂ is now defined as the sum of the eddy covariance, measured at a reference height, the storage term and horizontal and vertical advection terms^[8,16,19–22].

At present, there are three methods to rotate coordination, 2D-rotation, 3D-rotation, and planar fit. In this study, we deal with wind coordination by 3D-rotation. The first rotation sets $\bar{v} = 0$ by swinging the x and y -axes about the z -axis. The second rotation sets $\bar{w} = 0$ swinging the new x and z -axes about y so that the x -axis points in the mean streamline direction. The above double rotation aligns the x -axis with the

mean wind vector, but allows the y and z -axes to freely rotate about x . That is, there are an infinite number of anemometer rotations that simultaneously satisfy $\bar{v} = \bar{w} = 0$. McMillen (1988) suggests that (over land) a third sonic rotation be applied to remove this ambiguity by requiring that $\bar{vw} = 0$. In this step the new y and x -axes are rotated around x until the cross-stream stress becomes zero^[23].

2.3 Gap filling

Gaps in the long-term data records will occur as malfunction of instruments, calibration of system, and when the wind is blowing through a tower from an undesirable wind sector, when sensors are wet or when the measurements fail to meet pre-set acceptance criteria.

Now, the gap filling methods include mean diurnal variations of previous periods, and look-up tables for F_{NEE} during assorted meteorological conditions, and gap filling by nonlinear regressions. Here in this paper the gap filling methods of mean diurnal variations and nonlinear regression are applied. In the mean diurnal variation, a missing observation is replaced by the mean for that time period based on adjacent days. The methods for derivation of diurnal pattern differ mainly in the length of the time interval of averaging (window size, usually 4–15 days). In addition, recent work on spectral analysis of flux data showed a spectral peak at 3–4 days, clear evidence not to use this period for averaging^[24]. Larger window sizes were not considered for carbon fluxes, as nonlinear regression on environmental variables introduces errors through averaging. In this paper, we used the 14-day independent windows during daytime, 7-day during night^[25]. In addition to the two interval lengths, two different algorithms were implemented: (1) an independent window, for each subsequent period of data (where the period length is defined by the window size) mean diurnal variations were established to fill gaps within that period; and (2) a gliding window, a window of prescribed size around each gap is used to construct mean diurnal variation for gap filling within that window.

3 Results and discussion

3.1 Seasonal variation of meteorology factor

Figure 1 shows that in the year 2003, except May and August, the monthly precipitation were all less than the mean level in the past, especially only 3.2 mm rainfall in July. The total precipitation of the year 2003 was about 60% of the mean precipitation in the past. Accordingly, the temperature was higher than the mean temperature significantly, especially 31.2°C in July, which was 2.4°C higher than the mean value for the past July since recording. Consequently, the maximum of monthly temperature sum occurred in July 2003. The year 2003 was a most serious drought year in the history for this region, especially in July.

3.2 Environment controls on NEE

(i) Light. NEE is the carbon flux occurring for a relatively long time; negative NEE shows the downward flux, positive NEE means upward flux. The whole day was divided into two parts according to the PAR, i.e. daytime for PAR > 0 and nighttime for PAR < 0. The response of NEE to PAR could be described as a rectangular hyperbola curve, always is the Michaelis-Menten model^[26].

$$F_{\text{NEE}} = \frac{\alpha \cdot \text{PPFD} \cdot P_{\text{max}}}{\alpha \cdot \text{PPFD} + P_{\text{max}}} - R_d, \quad (10)$$

where F_{NEE} ($\text{mgCO}_2 \cdot \text{m}^{-2} \cdot \text{s}^{-1}$) is net ecosystem exchange in daytime, α ($\text{mgCO}_2 \cdot \text{m}^{-2} \cdot \text{s}^{-1} / \mu\text{mol photons} \cdot \text{m}^{-2} \cdot \text{s}^{-1}$) the quantum yield, P_{max} the

canopy-scale photosynthetic rate at the saturate light level, R_d the daytime ecosystem respiration.

Since February, PAR was becoming stronger and stronger for the increasing solar height angle; it reached the maximum in July, and then decreased until February next year. The NEE was influenced by leaf assimilation, so the plant physiological activity became more and more vigorous as PAR increasing, and then weaker and weaker as the solar height angle decreasing. The photosynthesis at the light-saturated point showed that the NEE increased from March and reached its peak in May, then decreased from then on, which was mainly caused by the serious drought in July. Similarly, apparent initial quantum efficiency increased from February, and reached its maximum in June, then decreased for the drought. The apparent initial quantum efficiency was 0.0204–0.0626 at 23 m height; with nadir in March, and maximum in June (for the instrument malfunction, the data in December and July could not be simulated, so the parameters was void), and in the intensive growing period (from April to October), it was around 0.0379. The apparent initial quantum efficiency was 0.0095–0.063 at the height of 39 m, with minimum in December and maximum in June, and 0.0428 in the strong growing season (Table 1).

The dependence of daytime CO₂ exchange on light for each month is presented in fig. 2(a), however, when the PAR attained a certain range, the NEE values became scatter, and the response to PAR reached the saturation when the PAR exceeded 1200 $\mu\text{mol} \cdot$

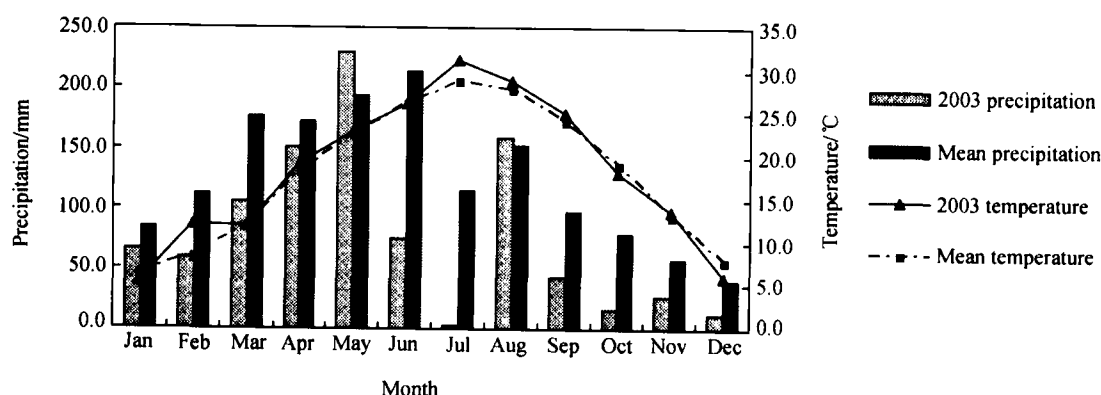


Fig. 1. Monthly precipitation and temperature in 2003.

Table 1 The function parameters for the response of monthly NEE to PAR (NEE and $R_d/\text{mg} \cdot \text{m}^{-2} \cdot \text{s}^{-1}$)

Month	23 m			39 m		
	α	NEE_{\max}	R_d	α	NEE_{\max}	R_d
January	0.0275	0.9438	0.0917	0.0197	0.7752	0.0443
February	0.0488	0.9186	0.1497	0.0329	0.5786	0.0969
March	0.0204	1.2330		0.0163	1.3260	
April	0.0316	1.1619	0.1046	0.0252	1.1893	0.0879
May	0.0245	1.7155	0.0422	0.0370	1.4560	0.1625
June	0.0627	1.1529	0.2665	0.0603	1.3254	0.2868
July				0.0508	0.7494	0.2846
August	0.0430	0.7796	0.1608	0.0304	0.9024	
September	0.0277	1.2400	0.1588	0.0297	1.1500	
October	0.0269	0.9844	0.0888	0.0214	1.1210	0.0816
November	0.0242	0.7115	0.0514	0.0197	0.6577	0.0348
December				0.0095	0.9539	0.0242
April to October	0.0379	0.9848	0.1437	0.0428	0.9498	0.1886

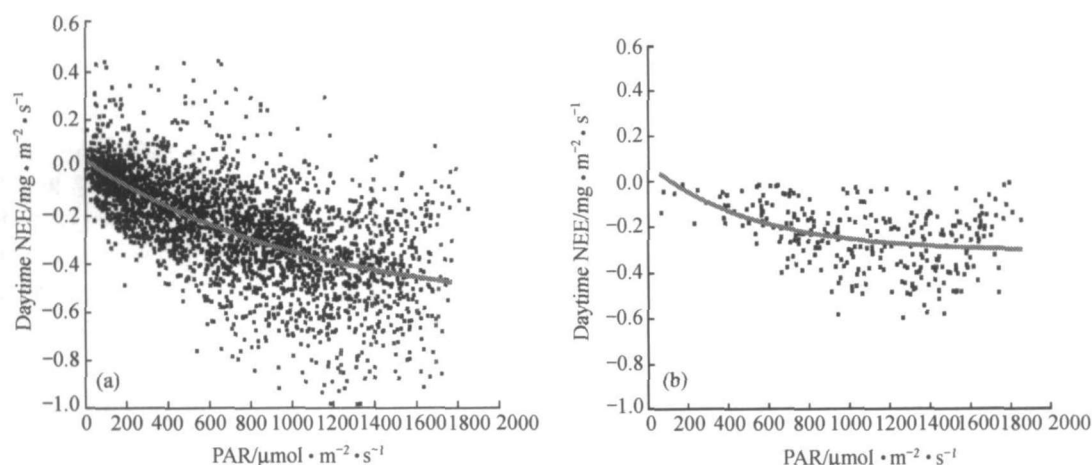


Fig. 2. The response of NEE to PAR. (a) The relationship between NEE and PAR in the whole year; (b) the relationship in the drought July.

$\text{m}^{-2} \cdot \text{s}^{-1}$. Fig. 2(b) shows that under the water stress, NEE could easily reach its saturated point with abundant radiation, and the daily maximum NEE value was less than that in the natural condition.

(ii) Friction velocity. There are many points for the underestimate of nighttime flux. Currently, the friction velocity was used as quality control for nighttime data. Aubinet's research showed that the relationship between carbon flux and temperature was distinct exponential function after the carbon flux was filtrated with the certain low threshold^[27]. Therefore, the friction velocity thresholds for nighttime data rejection were established^[2,28–31]. The threshold friction velocity used in this study is $0.2 \text{ m} \cdot \text{s}^{-1}$, as the NEE

increased with friction velocity.

(iii) Temperature. It is a significant exponential relationship between soil respiration in nighttime and temperature^[32]. Also, the relationship between them was studied in this paper. Fig. 3 shows that the regression could be described as the following equation when friction velocity was larger than $0.2 \text{ m} \cdot \text{s}^{-1}$:

$$NEE(n) = 0.0279 \exp(0.0707T_{s_{5\text{cm}}}).$$

The soil respirations were scattered according to soil temperature, but were relatively concentrated in the range of low temperature. In the range of $15\text{--}25^\circ\text{C}$, the Q_{10} was 1.9. Accordingly, the exponential relationship between soil respiration and soil heat flux

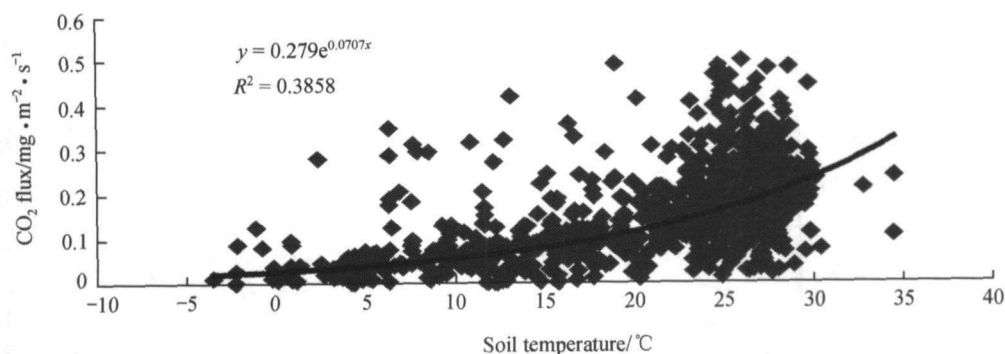


Fig. 3. The response of carbon flux in nighttime to soil temperature.

was also significant during nighttime when the friction velocity was higher than $0.2 \text{ m} \cdot \text{s}^{-1}$, especially at the depth of 3 cm. The function was

$$\text{NEE}(n) = 0.1163 \exp(0.0578 G_{s3 \text{ cm}}).$$

In summary, the relationship between respiration and temperature is identical to the previous study^[25,32] when the data was filtered using friction velocity threshold. The NEE during nighttime was determined by ecosystem respiration, and heat condition was its key impact factor. Therefore, air temperature under canopy, topsoil temperature and soil heat flux all govern the respiration rate, elevated temperature accelerate the metabolism of vegetation and soil microorganism, hence the carbon emission.

3.3 Monthly mean diurnal variation

The monthly diurnal variation at the height of 23 m is presented in fig. 4. Fig. 4(a) and (b) demonstrate the variation in weak growing seasons. Fig. 4(c) shows the variation in strong growing season, and fig. 4(d) indicates the variation in strong growing drought season. The curves showed that the changing trends were coincidence in the whole year; the carbon flux was positive during the nighttime (18:00—08:00), and negative at the other period. So the ecosystem shows a carbon source for the respiration at night, and a carbon sink for photosynthesis in the daytime. From the diurnal variation, the drastic fluctuations for carbon flux around sunrise and sunset were observed; they were caused by the atmosphere disturbance. The carbon flux increased in the morning, and reached its peak at noontime, which suggests that the trees were regulat-

ing their stomata to reduce water loss. In the weak growing seasons (January—March, November—December) the maximum of carbon flux was about -0.29 — $0.39 \text{ mg} \cdot \text{CO}_2 \cdot \text{m}^{-2} \cdot \text{s}^{-1}$, and in the intensive growing season it ranged from -0.40 to $-0.60 \text{ mg} \cdot \text{CO}_2 \cdot \text{m}^{-2} \cdot \text{s}^{-1}$. However, in July and August the vegetation growing was limited by water stress for drought, so that the carbon flux was less than that of other months. Consequently, the diurnal maximum of carbon flux reached the peak in the strong growing season, and the growing condition of vegetation directly controlled the carbon flux.

3.4 Seasonal variation

After filling the data gap in the whole year of 2003, and summing all the carbon flux monthly, we obtained the seasonal variation of NEE, as presented in fig. 5. Fig. 5 shows that the ecosystem was a carbon sink in the year 2003, so whether in the weak growing season or the strong growing season, the carbon input to the ecosystem was larger than the carbon output to the atmosphere. During the whole year, NEE reached its peaks in May and September, because of serious drought during June and July, the NEE was much less than that in other months among the strong growing season. The maximum of NEE was -290 to $-355 \text{ mg} \cdot \text{CO}_2 \cdot \text{m}^{-2} \cdot \text{month}^{-1}$, and the minimum was -144 to $-156 \text{ mg} \cdot \text{CO}_2 \cdot \text{m}^{-2} \cdot \text{month}^{-1}$.

The positive difference of NEE between 23 and 39 m indicated that the flux at 39 m was smaller than that at 23 m. Fig. 5 shows that the difference between

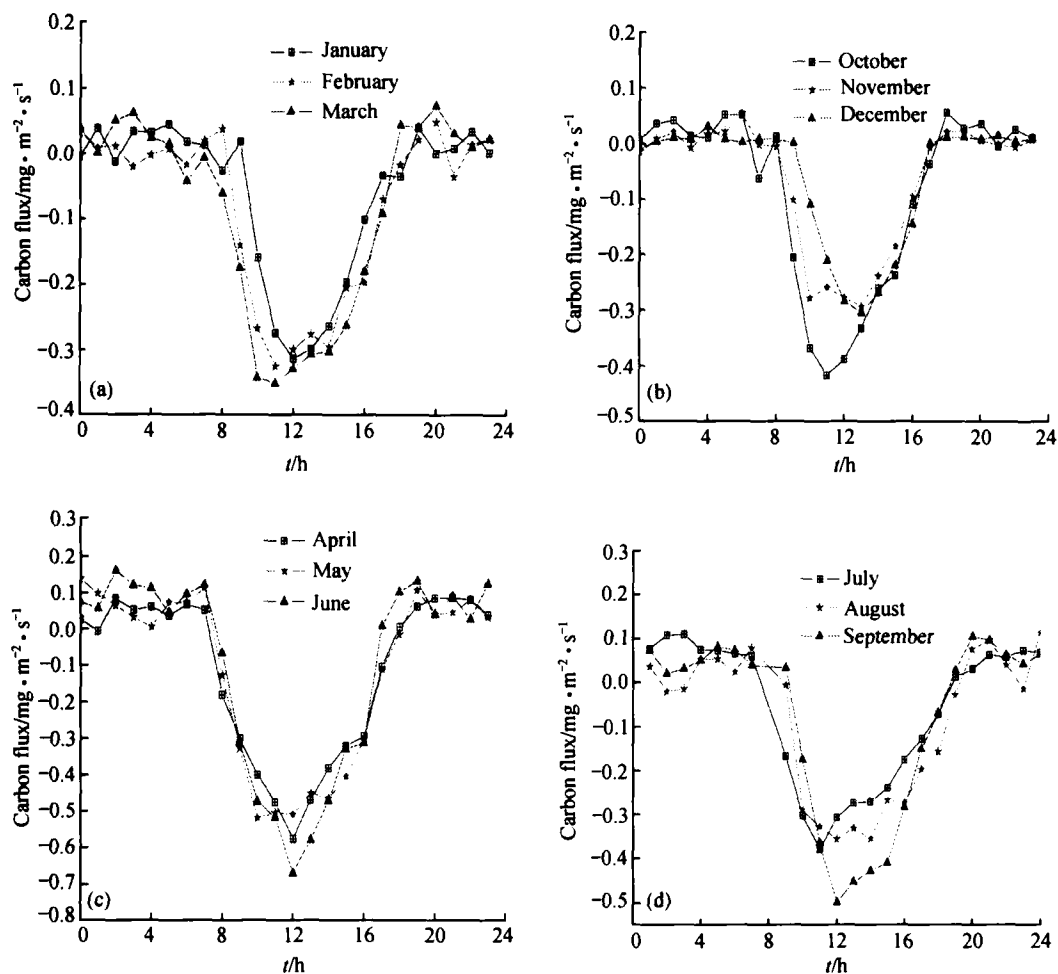


Fig.4. The carbon flux monthly diurnal variation at the height of 23 m (as the instrument malfunction, the data of July, August and September were used at the height of 39 m).

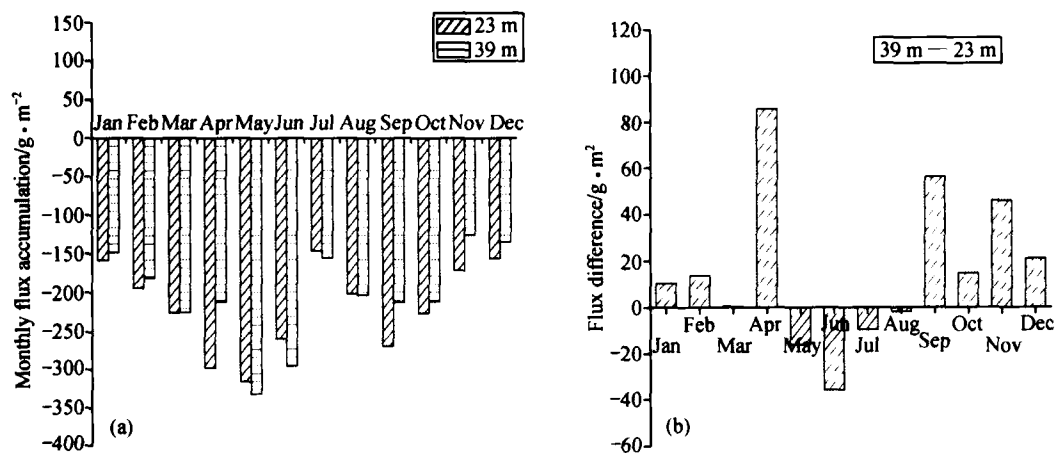


Fig. 5. Seasonal variation of NEE and the difference of the NEE at two heights.

the two heights reached its peaks in February and May, it was similar to that of the NEE in two heights; and only in September was NEE at 23 m smaller than at 39 m. The main controlling factors included the area and types of carbon sink or source, the vegetation growing condition, meteorological factors, and wind directions. The different wind directions resulted in different carbon sinks or sources, so that the difference of NEE at two different heights varied consequently, to which we should pay more attention.

3.5 Annual carbon sequestration estimation

Summing the half-hourly carbon flux measurement provided a rough estimation of the annual carbon sequestration by the ecosystem. However, this requires complete data series. To do so, all data gaps resulting from system failures, power cuts or using mean diurnal variation filled in data removal because of their bad quality. This procedure gives a first rough estimation of carbon sequestration as $-0.553 \text{ kgC} \cdot \text{m}^{-2}$ per year at the measurement height of 39 m, and $-0.645 \text{ kgC} \cdot \text{m}^{-2}$ at 23 m. This result shows that the ecosystem behaves as a carbon sink. Aubinet (2001) investigated the carbon budget of Belgian Ardennes mixed forest for $-0.60 \text{ kg} \cdot \text{m}^{-2} \cdot \text{per year}^{[33]}$, Peter M. Anthoni (1999) calculated a spare canopy ponderosa pine as $320 \pm 170 \text{ gC} \cdot \text{m}^{-2[34]}$. The results from this study was relatively large, the probable reason lies on the fast growing period for the studied forest.

4 Conclusions

This paper analyzed the effects of environmental factors over carbon flux, studied the seasonal and monthly diurnal variation, the spatial and temporal variation of carbon flux at the two heights of 23 m and 39 m, and the carbon sequestration of the ecosystem during the year 2003. The results showed that the monthly diurnal variation was significant. Then the first rough estimate of carbon sequestration about $-0.553 \text{ kg} \cdot \text{Cm}^{-2}$ per year at the measurement height of 39 m, and $-0.645 \text{ kg} \cdot \text{Cm}^{-2}$ at 23 m were brought out. The ecosystem was a carbon sink in the year 2003. The seasonal variation of NEE was obvious; and NEE was larger in the strong growing season than that in

the weak growing season, and water stress affected the magnitude of NEE. The seasonal variation of NEE difference between 23 m and 39 m was significant, resulting from the divergence or advection between the two heights. The carbon flux measured at 23 m every month was larger than that at 39 m, except for September. The regression equation between NEE and PAR in the daytime showed that there was an obvious seasonal variation of apparent initial quantum efficiency and P_{max} , and the values of them in the strong growing season were larger than that in the weak growing season. The exponential relationship was presented between soil temperature or soil heat flux and respiration in nighttime. PAR and soil temperature are two important factors strongly affecting NEE.

Acknowledgements This work was supported by the Chinese Academy of Sciences and the Ministry of Science and Technology (Grant Nos KZCX1-SW01 and 2002CB412500), and Institute of Geographic Sciences and Natural Resources Research, CAS, the Knowledge Innovation Engineering Backbone Science Plan, respectively. We also appreciate the technical assistance provided by Campbell Scientific Inc, USA, and its representative, the Tempo company in China.

References

1. Goulden, M. L., Daube, B. C., Fan, S. M. et al., Physiological response of a black spruce forest to the weather, *Journal of Geophysical Research*, 1997, 102: 28987—28996.
2. Black, T. A., Den, H. G., Neumann, H. H. et al., Annual cycles of water vapor and carbon dioxide fluxes in and above a boreal aspen forest, *Global Change Biology*, 1996, 2: 219—229.
3. Grace, J., Malhi, Y., Lloyd, J. et al., The use of eddy covariance to infer the carbon dioxide uptake of Brazilian rain forest, *Global Change Biology*, 1996, 2: 209—217.
4. Berbigier, P., Bonnefond, J. M., Mellmann, P., CO₂ and water vapor fluxes for 2 years above Euroflux forest site, *Agricultural and Forest Meteorology*, 2001, 108: 183—197.
5. Baldocchi, D., Finnigan, J., Wilson, K. et al., On measuring net ecosystem carbon exchange over tall vegetation on complex terrain, *Boundary-Layer Meteorology*, 2000, 96: 257-291.
6. Song, X., Liu, Y., Xu, X. et al., The comparison study on change dioxide, water and heat fluxes in winter and spring over the forest ecosystem in red earth hilly zone, *Recourses Sciences (in Chinese)*, 2004, 26(3): 96—104.
7. Baldocchi, D., Hicks, B., Meyers, P., Measuring biosphere-atmosphere exchanges of biologically related gases with micrometeorological methods, *Ecology*, 1988, 69: 1331—1340.
8. Paw, U. K., Baldocchi, D. D., Meyers, T. P. et al., Correction of eddy covariance measurements incorporating both advective effects and density fluxes, *Boundary-Layer Meteorology*, 2000, 97: 487-511.

9. Reynolds, O., On the dynamical theory of incompressible viscous fluids and the determination of criterion, *Phil. Trans. Roy. Soc. London A*, 1895, 174: 935—82.
10. Fan, S. M., Wofsy, S. C., Bakwin, P. S. et al., Atmosphere-biosphere exchange of CO₂ and O₃ in the central Amazon forest, *J. Geophys. Res.*, 1990, 95: 16851—16864.
11. Garratt, J. R., Limitations of the eddy correlation technique for determination of turbulent fluxes near the surface, *Bound.-Lay. Meteorol.*, 1975, 8: 255—259.
12. Webb, E. K., Pearman, G., Leuning, R., Correction of flux measurements for density effects due to heat and water vapor transfer, *Q. J. Roy. Meteorol. Soc.*, 1980, 106: 85—100.
13. Massman, W. J., Lee X., Eddy covariance flux corrections and uncertainties in long term studies of carbon and energy exchanges, *Agric. For. Meteorol.*, 2002, 113: 121—144.
14. Leuning, R., Moncrieff, J., Eddy covariance CO₂ flux measurements using open- and closed-path CO₂ analysers: corrections for analyzer water vapour sensitivity and damping of fluctuations in air sampling tubes, *Boun.-Lay. Meteorol.*, 1990, 53: 63—76.
15. Leuning, R., Judd, M. J., The relative merits of open and closed path analysers for measurement of eddy fluxes, *Global Change Biology*, 1996, 2: 241—253.
16. Finnigan, J. J., A comment on the paper by Lee (1998): "On micrometeorological observations of surface-air exchange over tall vegetation", *Agric. For. Meteorol.*, 1999, 97: 55—64.
17. McMillen, R. T., An eddy correlation technique with extended applicability to nonsimple terrain, *Boun.-Lay. Meteorol.*, 1988, 43: 231—245.
18. Foken, T., Wichura, B., Tools for quality assessment of surface-based flux measurements, *Agric. For. Meteorol.*, 1995, 78: 83—105.
19. Lee, X., On micrometeorological observations of surface-air exchange over tall vegetation, *Agric. For. Meteorol.*, 1998, 91: 39—50.
20. Sun, J., Desjardins, R., Mahrt, L. et al., Transport of carbon dioxide, water vapor and ozone by turbulence and local circulations, *J. Geophys. Res.*, 1998, 103: 25873—25885.
21. Yi, C., Davis, K., Bakwin, P. et al., Influence of advection on measurements of the net ecosystem-atmosphere exchange of CO₂ from a very tall tower, *J. Geophys. Res.*, 2000, 105: 9991—9999.
22. Eugster, W., Siegrist, F., The influence of nocturnal CO₂ advection on CO₂ flux measurements, *Basic and Applied Ecology*, 2000, 1: 177—188.
23. McMillen, R. T., An eddy correlation technique with extended applicability to non-simple terrain, *Boundary Layer Meteorology*, 1988, 43: 231—245.
24. Baldocchi, D. D., Falge, E., Wilson, K., A spectral analysis of biosphere-atmosphere trace gas flux densities and meteorological variables across hour to year time scales, *Agric. For. Meteorol.*, 2001, 107: 1—27.
25. Falge, E., Baldocchi, D., Olson, R., Gap filling strategies for defensible annual sums of net ecosystem exchange, *Agricultural and Forest Meteorology*, 2001, 107: 43—69.
26. Michaelis, L., Menten, M. L., Die Kinetik der Invertinwirkung, *Biochem Z.*, 1913, 49: 333.
27. Aubinet, M., Grelle, A., Ibrom, A. et al., Estimates of the annual net carbon and water exchange of European forests: the EUROFLUX methodology, *Adv. Ecol. Res.*, 2000, 30: 113—75.
28. Goulden, M. L., Crill, P. M., Automated measurements of CO₂ exchange at the moss surface of a black spruce forest, *Tree Physiol.*, 1997, 17: 537—542.
29. Jarvis, P. G. J. M., Massheder, S. E. Hale, J. B. et al., Seasonal variation of carbon dioxide water vapor, and energy exchanges of a boreal black spruce forest, *J. Geophys. Res.*, 1997, 102: 28953—28966.
30. Lindroth, A. A., Grelle, A., Moren, A. S., Long-term measurements of boreal forest carbon balance reveal large temperature sensitivity, *Global Change Biol.*, 1998, 4: 443—450.
31. Xuhui Lee, Long-term observation of the atmospheric exchange of CO₂ with a temperate deciduous forest in southern Ontario, Canada, *Journal of Geophysical Research*, 1999, 104, D13, 15975—15984.
32. Lloyd, J., Taylor, J. A., On the temperature dependence of soil respiration, *Funct. Eco.*, 1994, 8: 315—323.
33. Anthoni, P. M., Law, B. E., Unsworth, M. H., Carbon and water vapor exchange of an open-canopied ponderosa pine ecosystem, *Agric. For. Meteorol.*, 1999, 95: 115—68.
34. Anthoni, P., Law, B., Unsworth, M., Carbon and water vapor exchange of an open-canopied ponderosa pine ecosystem, *Agricultural and Forest Meteorology*, 1999, 95: 151—168.